

Self-supervised Likelihood Estimation with Energy Guidance for Anomaly Segmentation in Urban Scenes

Yuanpeng Tu^{1*} Yuxi Li^{2*} Boshen Zhang^{2*} Liang Liu² Jiangning Zhang²
Yabiao Wang² Chengjie Wang² Cai Rong Zhao¹

¹Dept. of Electronic and Information Engineering, Tongji Univeristy, Shanghai

²YouTu Lab, Tencent, Shanghai

{2030809, zhaocairong}@tongji.edu.cn

{yukiyxli, boshenzhang, leoneliu, vtzhang, caseywang, jasoncjwang}@tencent.com

Abstract

Robust autonomous driving requires agents to accurately identify unexpected areas in urban scenes. To this end, some critical issues remain open: how to design advisable metric to measure anomalies, and how to properly generate training samples of anomaly data? Previous effort usually resorts to uncertainty estimation and sample synthesis from classification tasks, which ignore the context information and sometimes requires auxiliary datasets with fine-grained annotations. On the contrary, in this paper, we exploit the strong context-dependent nature of segmentation task and design an energy-guided self-supervised frameworks for anomaly segmentation, which optimizes an anomaly head by maximizing the likelihood of self-generated anomaly pixels. For this purpose, we design two estimators for anomaly likelihood estimation, one is a simple task-agnostic binary estimator and the other depicts anomaly likelihood as residual of task-oriented energy model. Based on proposed estimators, we further incorporate our framework with likelihood-guided mask refinement process to extract informative anomaly pixels for model training. We conduct extensive experiments on challenging Fishyscapes and Road Anomaly benchmarks, demonstrating that without any auxiliary data or synthetic models, our method can still achieves competitive performance to other SOTA schemes.

1. Introduction

Recent studies in semantic segmentation have achieved significant advance on close-set benchmarks of urban scenarios [10]. However, when it comes to deployment in the wild, it is necessary to enable segmentation models with the ability of anomaly detection, *i.e.*, to ensure segmenta-

* Yuanpeng Tu, Yuxi Li, Boshen Zhang contribute equally to this work.

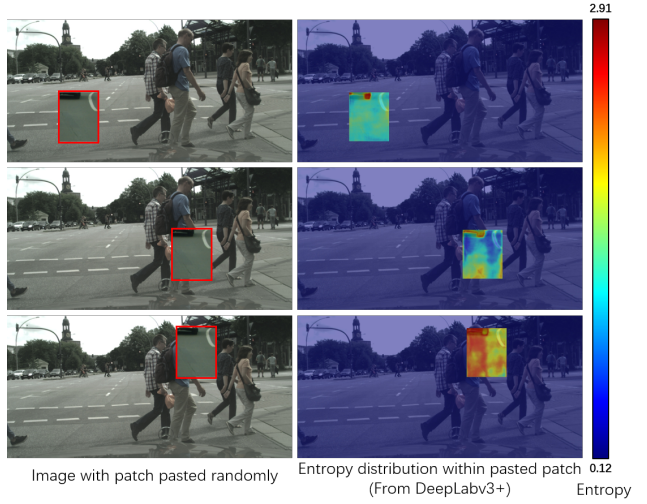


Figure 1. Illustration of contextual reliance in anomaly segmentation tasks. The **left** column shows an image pasted with a random patch at different position. The **right** column illustrates the corresponding entropy distribution from segmentation results of DeepLab segmentation model [9]. Different pasted positions result in various uncertainty distribution within the patch.

tion networks can identify some Out-of-Distribution (OoD) objects which did not appear in its training set.

Essentially, the key of segmentation with anomalies lies in two aspects: *Firstly*, the anomaly score should be carefully designed to effectively differentiate anomaly pixels and normal ones. *Second*, other than normal data from segmentation datasets, extra anomaly data is critical to explicitly identify which pixel belongs to unexpected objects. To address these issues, a fresh wave of approaches in semantic segmentation are proposed recently. To measure the likelihood of anomalies, some methods take insight from uncertainty estimation and devise a series of proxy tasks [17, 22, 34, 35, 41]. However, these approaches usually design coupled objective for both segmentation and anomaly detection, and require retraining of segmentation models, which

might degrade the performance on both tasks [6]. On the other hand, to generate training samples with anomaly pixels, outlier exposure is widely adopted [2, 8, 17] with auxiliary data, while in a practical sense, these methods increase the cost due to additional labeling requirements, the adopted OoD data is also not guaranteed to be consistent with realistic scenes. There are also approaches leveraging an extra well-trained reconstruction model and taking the difference as anomaly parts [13, 42, 43], which inevitably affect the efficiency and the detection results highly rely on the reconstruction quality.

By summary, most of previous effort tends to take insight from OoD modeling in traditional classification tasks. Nevertheless, semantic segmentation differs since the segmentation results inherently rely on its spatial context. As shown in Fig. 1, when placed under different context in the image, the same patch yield different semantic uncertainty (measured as the entropy of categorical distribution) for a given semantic segmentation model [9], even though the patch is filled with In-Distribution (ID) pixels. The empirical observation from Fig. 1 inspires that we can simply synthesize anomaly objects from ID data with a self-supervised copy-and-paste manner. However, vanilla paste operation cannot always accurately resemble anomaly objects. Therefore, in this paper, we propose a new framework termed as **Self-supervised Likelihood Estimation with Energy Guidance (SLEEG)**, which extends off-the-shelf segmentation models to anomaly detectors while avoiding the overhead of labeling auxiliary data with the guidance of energy-based model [27].

The SLEEG framework is designed in a self-teaching paradigm, to properly depict the anomaly area, we derive two anomaly likelihood estimators based on predicted joint probability of content and anomalies. The first is formulated as a simple task-agnostic classifier to differentiate anomaly and normal pixels. The other is a task-oriented estimator and can be naturally regarded as residual estimation of classic negative joint-energy modeling (JEM) [16], with proper design of loss function, this estimator can be optimized through a dynamic energy-guided margin. Next, based on these estimators, we design an adaptive refinement mechanism to provide more representative OoD patches, which is guided by anomaly likelihood estimated on each pixel.

We implemented SLEEG with different segmentation models and evaluate the performance on benchmarks of Fishyscapes [4] and Road Anomaly [7]. Experiments results show that SLEEG can bring consistent improvement over different baselines by training with only ID dataset of Cityscapes [10]. Further, compared with state-of-the-art anomaly segmentation methods, SLEEG achieves competitive results **without training on labeled OoD data or updating parameters of segmentation networks**. In summary, the contributions of this paper can be listed as:

- We propose SLEEG, a self-supervised framework for anomaly segmentation with a copy-and-paste manner. In the framework, we design two decoupled likelihood estimators from energy model, a task-agnostic estimator for discriminative learning and a task-oriented estimator for residual learning of joint-energy.
- Based on the proposed energy-guided estimators, we propose a dynamic mask refinement mechanism by applying likelihood-guided pixel separation to help extract more informative OoD pixels for training.
- Without training on labeled OoD data or updating segmentation parameters, our SLEEG achieves competitive performance on both Fishyscapes [4] and Road Anomaly [7] benchmarks.

2. Related Work

2.1. Out of Distribution Detection

Out of distribution (OoD) detection focuses on distinguish test samples of a different distribution from the training set, which can be considered as a two-class classification task. Existing OoD detection methods can be roughly divided into four categories: classification-based [12, 23], density-based [29, 47], distance-based [29, 40] and reconstruction-based [44, 46], *etc.* Although classical OoD detection methods can achieve high accuracy on classification tasks, poor performance is obtained when directly applying them to anomaly segmentation tasks since they ignore the context of pixels [6].

2.2. Anomaly Segmentation

Uncertainty Estimation. Similar to image-level anomaly detection approaches, early uncertainty based methods [21, 28] focused on measuring anomaly scores of each pixel with maximum softmax probability produced by the softmax classifier since the model tends to output uniform prediction for unseen semantics. However, they are prone to misclassify pixels of tail classes as anomalies, since the same threshold is set for all pixels regardless of the class-wise distribution discrepancy. To address this issue, Jung *et al.* [25] proposed standardized max logit (SML), which normalized the distribution of max logit from seen classes and mitigates the influence of anomalous boundary pixels with neighboring-pixel iterative refinement, bringing considerable improvement. [26] attempted to tackle this problem with MC dropout while achieving marginal boost. Recent methods try to enhance ability of distinguishing hard samples from anomalous ones by re-training the whole framework or utilizing extra OoD data. However, these approaches generally suffer from accuracy decrease on seen categories [6]. Chan *et al.* [8] utilized objects of COCO datasets [31] as OoD samples in Cityscapes and performed

pixel-wise anomalous class predictions by incorporating an extra meta classifier to make models more sensitive to unexpected objects. However, in real-world scenarios, the appeared unexpected objects are always unable to be accessed.

Image Reconstruction. Methods based on image reconstruction [32, 43] usually employ generative adversarial networks (GANs) [11] to fit the distribution of normal pixel data, re-synthesize images conditioned on predicted segmentation results and localize the discrepancy between original images and reconstructed ones as anomalous objects. Nevertheless, these approaches usually heavily rely on the accurate segmentation maps and performance of reconstruction model, while it is difficult for the segmentation models to distinguish hard in-distribution pixels and OOD ones. On the other hand, their performance can be affected by the artifacts generated by GANs as well. Finally, they also suffer from time-consuming serialized training and inference processes of the reconstruction networks, making them hard to be applied in real-time scenarios [6].

Outlier Exposure. Recent promising methods [1, 2, 8, 14, 23] are intuitive, which utilize samples from non-overlapped classes of an external auxiliary dataset as outliers to help models differentiate unexpected instances against in-distribution pixels. Hendrycks et al. [23] firstly tried to impose outlier exposure on anomaly detection to boost the performance. Petra et al. [1] exploited objects from the large-scale ImageNet [38] with bounding boxes as OoD samples to perform dense anomalous predictions, while [8] and [14] leveraged COCO [31] with instance masks and void class map of Cityscapes [10] as outliers respectively to make model generalize to unseen objects. However, they usually require re-training of the whole segmentation model and suffer from potential degradation in accuracy of in-distribution recognition by maximizing uncertainty of outliers. Besides, these strategies require fine-grained annotation of unexpected objects in OoD images, inevitably increasing the cost of labeling. Finally, utilizing specific auxiliary datasets as outliers may lead the anomaly detection algorithms biased toward certain domain, resulting in accuracy deterioration in real-world applications.

2.3. Energy Based Modeling

There is also a special series of methods applying energy function [27] to depict probabilities of OoD data. These approaches focus on minimizing energy for inlier training instances while maximizing energy for unseen outlier samples. Afterwards, the energy value is taken as measurement to predict anomaly probability of samples. Previous energy-based models generally employ Markov Chain Monte Carlo as the partition function to estimate energy score whereas high-quality samples cannot be generated in this manner. To address this issue, [41] simply utilizes the joint-energy [16] with additional smooth terms to help the absented learning

of models, while still requiring outlier exposure strategy.

3. Methodology

In this section we introduce the detail of SLEEG framework, which is depicted as Fig. 2. Given an image $\mathcal{I} \in \mathbb{R}^{3 \times H \times W}$ with H, W indicating its spatial resolution, its spatial coordinate set is defined as Ω , we associate the pixel x_ω at each coordinate $\omega \in \Omega$ with a triplet variable $(z_\omega, y_\omega, o_\omega)$, where $z_\omega \in \mathbb{R}^D$ represents the encoded feature of dimension D , $y_\omega \in \{0, 1, \dots, K-1\}$ denotes predicted categorical labels over K close-set semantic classes, and $o_\omega \in \{0, 1\}$ is a binary indicator to denote whether x_ω belongs to anomaly. Our approach follows the classical Encoder-Decoder meta-architecture in semantic segmentation, where an encoder $\mathcal{F}_\Phi(\cdot) : \mathbb{R}^{3 \times H \times W} \rightarrow \mathbb{R}^{D \times H \times W}$ extracts deep features and a segmentation decoder $g_\phi(\cdot) : \mathbb{R}^D \rightarrow \mathbb{R}^K$ is responsible to predict categorical distribution, both Φ, ϕ can be pretrained parameters from off-the-shelf segmentation models.

3.1. Joint Likelihood Estimation of Anomaly

For the ease of derivation, we recap the energy-based model [16, 27] by taking the decoder as an energy function, which is utilized to estimate joint distribution $p(z_\omega, y_\omega)$

$$z_\omega = \mathcal{F}_\Phi(\mathcal{I})_\omega \quad p(z_\omega, y_\omega) = \frac{1}{\mathcal{T}(\phi)} \exp(g_\phi(z_\omega))[y_\omega] \quad (1)$$

where $[y_\omega]$ is the y_ω -th index of output categorical vector, and $\mathcal{T}(\phi) = \int_{z_\omega} \sum_{y_\omega} \exp(g_\phi(z_\omega))[y_\omega] dz_\omega$ is an unknown normalization factor. With the formulation in Eq. (1), the probability $p(y_\omega|z_\omega)$ can be obtained via Bayes Rule.

The probability estimation above can only describe the relationship between content and semantics, hence we further extend a similar lightweight decoder $h_\theta(\cdot) : \mathbb{R}^D \rightarrow \mathbb{R}^2$ (termed as OoD head) from original segmentation model to depict the joint likelihood of $p(z_\omega, o_\omega)$

$$p(z_\omega, o_\omega) = \frac{1}{\Gamma(\theta)} \exp(h_\theta(z_\omega))[o_\omega] \quad (2)$$

where $\Gamma(\theta)$ is another constant factor similar to $\mathcal{T}(\phi)$. With this definition, our goal is to maximize the likelihood $p(o_\omega = 1|z_\omega)$ of pixels from anomaly while minimize those from normal pixels. To this end, we also resort to the Bayes Rule, however, since the feature encoding z_ω is jointly modeled with both semantic and anomaly, the likelihood function can be derived with different marginalization

$$p(o_\omega|z_\omega) = \frac{p(z_\omega, o_\omega)}{\sum_{o_\omega=0}^1 p(z_\omega, o_\omega)} = \frac{p(z_\omega, o_\omega)}{\sum_{y_\omega=1}^K p(z_\omega, y_\omega)} \quad (3)$$

By observation of Eq. (3), the first modeling only focus on differentiating anomalies regardless of segmentation task,

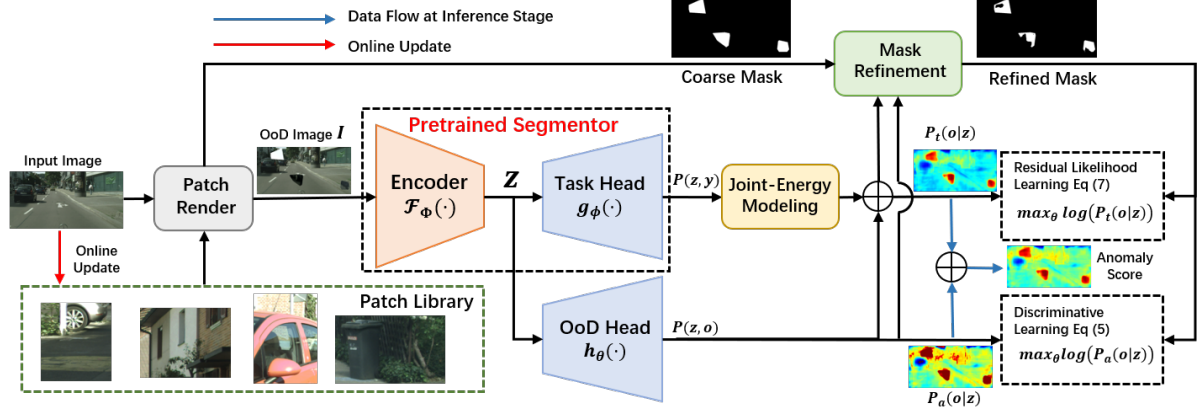


Figure 2. Illustration of proposed SLEEG framework, an OoD head is extended and trained in a self-supervised manner to enable a pretrained segmentation model with anomaly detection ability.

while the other takes semantic distribution into consideration. This inspires us to design two estimators to describe anomaly likelihood and optimize them respectively.

Task Agnostic Estimator (TAE). By taking the anomaly segmentation as pixel-wise binary classification problem, we can easily derive the likelihood from Eq. (2) and Eq. (3) with the normalization factor $\Gamma(\theta)$ eliminated

$$p_a(o_\omega | z_\omega; \theta) = \frac{\exp(h_\theta(z_\omega))[o_\omega]}{\sum_{o_\omega \in \{0,1\}} \exp(h_\theta(z_\omega))[o_\omega]} \quad (4)$$

Since Eq. (4) is a normalized probability function, we can optimize this estimator via simple cross-entropy loss

$$\mathcal{L}_a(\theta) = -E_{x_\omega \in \mathcal{S}_{ood}} [\log p_a(o_\omega = 1 | z_\omega; \theta)] - E_{x_\omega \in \mathcal{S}_{id}} [\log p_a(o_\omega = 0 | z_\omega; \theta)] \quad (5)$$

where \mathcal{S}_{ood} denote the set of anomaly pixels and \mathcal{S}_{id} is the set of normal pixels.

Task Oriented Residual Estimator (TORE). When taking joint probability $p(z_\omega, y_\omega)$ from Eq. (1) for marginalization in Eq. (3), the estimated likelihood $p_t(o_\omega | z_\omega; \theta)$ is coupled with constants $\Gamma(\theta)$ and $\mathcal{T}(\phi)$, which is intractable, hence we transform the likelihood into logarithmic form

$$\log p_t(o_\omega | z_\omega; \theta) = h_\theta(z_\omega)[o_\omega] + \text{JEM}(z_\omega) + C(\phi, \theta) \quad (6)$$

$$\text{JEM}(z_\omega) = -\log \sum_{y_\omega} \exp(g_\phi(z_\omega))[y_\omega]$$

Note that the second term in Eq. (6) is exactly the negative joint-energy model (JEM) [16] in uncertainty estimation and $C = \log(\mathcal{T}(\phi)/\Gamma(\theta))$ is a constant factor, therefore Eq. (6) essentially takes decoder h_θ to estimate the residual of JEM score, which is coarse estimation of anomaly. To optimize the estimator while handling intractable factor C , we propose to exploit a margin loss to compare the likelihood of anomaly and normal pixels

$$\mathcal{L}_o(\theta) = \{E_{x_\omega \in \mathcal{S}_{id}} [\log p_t(o_\omega = 1 | z_\omega; \theta)] - E_{x_{\omega'} \in \mathcal{S}_{ood}} [\log p_t(o_{\omega'} = 1 | z_{\omega'}; \theta)] + \gamma\}_+ \quad (7)$$

where γ is a hyperparameter to control the margin, $\{\cdot\}_+$ indicates truncating the value to 0 if it is negative. Note that the loss term in Eq. (7) can be reformulated as

$$\mathcal{L}_o(\theta) = \{E_{x_\omega \in \mathcal{S}_{id}} [h_\theta(z_\omega)] - E_{x_{\omega'} \in \mathcal{S}_{ood}} [h_\theta(z_{\omega'})] + \hat{\gamma}\}_+ \quad (8)$$

$$\hat{\gamma} = \gamma + E_{x_\omega \in \mathcal{S}_{id}} [\text{JEM}(z_\omega)] - E_{x_{\omega'} \in \mathcal{S}_{ood}} [\text{JEM}(z_{\omega'})]$$

therefore, different from other methods directly optimizing JEM [17, 41], the optimization of TORE can be regarded as taking estimated joint-energy to dynamically control the margin $\hat{\gamma}$ of anomaly confidence from h_θ for each image.

Finally, the predicted anomaly score can be expressed as the combination of both estimators

$$\mathcal{A}(x_\omega) = \log p_a(o_\omega | z_\omega; \theta^*) + \lambda \log p_t(o_\omega | z_\omega; \theta^*) \quad (9)$$

where λ is a balance factor and θ^* denotes the parameters of OoD head after optimization.

3.2. Self-supervised Training with Refined Patch

In this section we describe our self-training pipeline, which is illustrated in Fig. 2. Different from classical outlier exposure [3, 13], we aim at generating training samples with both anomaly pixels \mathcal{S}_{ood} and normal area \mathcal{S}_{id} in a self-supervised manner from coarse to fine.

Anomaly Patch Rendering. Intuitively, due to the contextual reliance of segmentation network, a random patch can be an anomaly part once placed under somewhat unnatural pattern, even if the patch is cropped from an in-distribution image. With this consideration, we design a dynamic copy-and-paste strategy to generate pseudo anomaly samples. In detail, we maintain a patch library during the whole training process, at each iteration, the library is updated with a randomly cropped patch from input normal images. Simultaneously, for each normal image, we randomly choose N patches as candidate anomalies. To make sure the

for simplicity, we ignore the index value $o_\omega = 1$ here

pasted patch yield more diverse geometry and more similar to real anomaly objects, we extracted the Harris corner points [18] and generate additional random points within the patch, and crop the minimum polygon containing all these points as anomaly patch, finally, all polygons from selected N patches are randomly pasted on input image.

Adaptive Mask Refinement. A naive way of self-supervised learning is to generate binary masks by taking all pixels within pasted patches as OoD set \mathcal{S}_{ood} for ground-truth. Nevertheless, as these patches are randomly cropped and pasted at random places, they can still contain objects which manifests complete in-distribution semantics and fits the context well. Taking these pixels as anomaly will reversely hinder the detection results. Therefore, to fully leverage the contextual information, we propose to take the estimated anomaly likelihood as guidance to further refine the pasted masks. Formally, we define the coordinates set of the i -th pasted polygon area as Ω_i^p , we aim at finding a threshold η to separate out pixels more likely to be anomaly

$$\mathcal{S}_{ood} = \{x_\omega | \omega \in \cup_{i=1}^N \Omega_i^p \wedge \mathcal{A}(x_\omega) \geq \eta\} \quad (10)$$

To properly refine the pasted patch, we design the threshold η^* in dynamic manner such that two separated pixel clusters in pasted area manifests minimum variance of anomaly scores within each group

$$\begin{aligned} \eta^* &= \arg \min_{\eta} Var_{x_\omega \in \mathcal{S}_{ood}}[\mathcal{A}(x_\omega)] + Var_{x_\omega \notin \mathcal{S}_{ood}}[\mathcal{A}(x_\omega)] \\ \text{s.t. } &\omega \in \cup_{i=1}^N \Omega_i^p \quad \min_{\omega} \mathcal{A}(x_\omega) \leq \eta \leq \max_{\omega} \mathcal{A}(x_\omega) \end{aligned} \quad (11)$$

The problem in Eq. (11) is non-differentiable for η , thus we transform it into discrete optimization by searching the optimal η^* in a grid scanning manner such that the gap between mean values of clusters is maximized [36]. After the refinement, the pasted areas not attributed to \mathcal{S}_{ood} is labeled as ignored and will not be used for loss computation. On the other hand, we take all pixels outside the pasted area as normal set \mathcal{S}_{id} . Fig. 3 shows some examples of refinement after our scheme, it can be clearly recognize that some part fitting the context well is automatically filtered out and other areas that are more contradictory to context are left for training. With the set separation above, we can reversely apply Eq. (5) and Eq. (7) to train the OoD head in a self-supervised paradigm.

4. Experiments

4.1. Experiments Settings

4.1.1 Datasets

Three anomaly datasets are included in our experiment: FishyScapes (FS) Lost & Found [5], FishyScapes (FS) Static [5] and Road Anomaly [7].

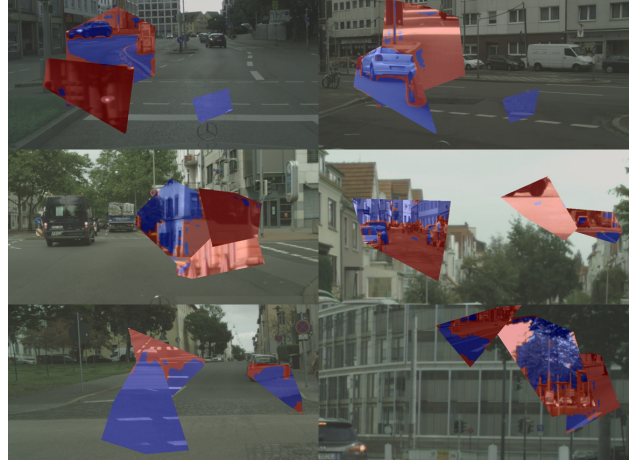


Figure 3. Visualization of generated patches with random shapes on training set of Cityscapes. Area with red mask denotes anomaly pixels after mask refinement, the blue area represents the ignored pixels from pasted patches.

FS Lost & Found is a widely-used anomaly segmentation dataset with high-resolution samples for autonomous driving scenes. FS Lost & Found is built based on the Lost & Found [37] and adopts the same collection setup as Cityscapes [10], which is also a segmentation benchmark for urban scenes. Specifically, 37 types of unexpected real road obstacles and 13 different street scenarios are included. Moreover, FS Lost & Found provides refined per-pixel annotations, including three classes: 1) unexpected obstacles, 2) objects with pre-defined classes in Cityscapes, 3) void regions. A validation set of 100 samples is publicly available, while the hidden test set with 275 images is entirely unknown. All the methods need to submit the code to the website to evaluate on this test set.

FS Static is artificially built upon the validation set of Cityscapes, where unexpected objects are collected from the Pascal VOC dataset [15] with the provided pixel-wise masks and positioned randomly on the underlying images. Specifically, only objects not belonging to the pre-defined classes of Cityscapes are used. This datasets consists of a public validation set with 30 images and a hidden test set with 1,000 images.

Road Anomaly includes 110 real-world images collected online (10 for validation and the other for online test), where anomalous obstacles (*e.g.*, animals, trash cans, etc) encounter on or locate near the road. All the images are rescaled to a size of $1,280 \times 720$ and pixel-wise annotations of unexpected objects are provided as well. Anomalous objects with various sizes are included, making the anomaly segmentation task on this dataset more challenging. Moreover, since there exists a larger domain gap between Road anomaly and Cityscapes, generalization ability of models is essential to the performance on this dataset.

Method	OoD Data	Re-training	FS LAF		FS Static	
			FPR ₉₅ ↓	AP ↑	FPR ₉₅ ↓	AP ↑
Synboost [13]	✓	✗	15.79	43.22	18.75	72.59
Density - Logistic Regression [5]	✓	✓	24.36	4.65	13.39	57.16
Bayesian Deeplab [35]	✗	✓	38.46	9.81	15.50	48.70
OoD Training - Void Class [5]	✓	✓	22.11	10.29	19.40	45.00
Discriminative Outlier Detection Head [3]	✓	✓	19.02	31.31	0.29	96.76
Dirichlet Deeplab [34]	✓	✓	47.43	34.28	84.60	31.30
DenseHybrid† [17]	✓	✓	6.18	<u>43.90</u>	5.51	72.27
PEBAL† [14]	✓	✓	<u>7.58</u>	44.17	<u>1.73</u>	<u>92.38</u>
MSP [22]	✗	✗	44.85	1.77	39.83	12.88
Entropy [22]	✗	✗	44.83	2.93	39.75	15.41
Density - Single-layer NLL [5]	✗	✗	32.90	3.01	21.29	40.86
kNN Embedding - density [5]	✗	✗	30.02	3.55	20.25	44.03
Density - Minimum NLL [5]	✗	✗	47.15	4.25	17.43	62.14
Image Resynthesis [33]	✗	✗	48.05	5.70	27.13	29.60
SML [25]	✗	✗	21.52	31.05	19.64	53.11
GMMSeg [30]	✗	✗	6.61	55.63	<u>15.96</u>	76.02
SLEEG (ours)	✗	✗	<u>6.69</u>	59.66	10.49	<u>68.93</u>

Table 1. Comparison with previous methods on the FS test set. “OoD Data” indicates training with additional labeled data. “Re-training” means updating parameters of segmentation network. † indicates training with WideResNet38 backbone. **Bold** values and underlined values represent the best and second best results. The comparison is conducted within each group.

Method	FS LAF Validation			FS Static Validation			Road Anomaly Test		
	FPR ₉₅ ↓	AUROC ↑	AP ↑	FPR ₉₅ ↓	AUROC ↑	AP ↑	FPR ₉₅ ↓	AUROC ↑	AP ↑
MSP [22]	45.63	86.99	6.02	34.10	88.94	14.24	68.44	73.76	20.59
MaxLogit [20]	38.13	92.00	18.77	28.50	92.80	27.99	64.85	77.97	24.44
SynthCP [43]	45.95	88.34	6.54	34.02	89.90	23.22	64.69	76.08	24.87
SML [25]	14.53	96.88	36.55	16.75	96.69	48.67	49.74	81.96	25.82
LDN_BIN [3]	23.97	95.59	45.71	-	-	-	-	-	-
GMMSeg [30]	13.11	97.34	43.47	-	-	-	47.90	84.71	34.42
Synboost [13]‡	34.47	94.89	40.99	47.71	92.03	48.44	59.72	85.23	41.83
DenseHybrid†‡ [17]	<u>6.10</u>	-	<u>63.80</u>	4.90	-	60.00	62.25	-	42.05
PEBAL†‡ [41]	4.76	98.96	58.81	1.52	99.61	92.08	<u>44.58</u>	<u>87.63</u>	<u>45.10</u>
SLEEG (ours)	10.90	<u>98.30</u>	70.90	<u>3.85</u>	<u>99.22</u>	<u>77.23</u>	36.40	89.00	52.70

Table 2. Comparison on FS validation sets and Road Anomaly. “‡” indicates the method adopts additional labeled data as OoD for training. † indicates training with WideResNet38 backbone. For DenseHybrid, we report the updated results from Road Anomaly Leaderboard under the similar segmentation setting. **Bold** values and underlined values represent the best and second best results.

We also evaluate the proposed method on a more challenging real-world anomaly segmentation dataset, Lost & Found [37]. State-of-the-art performance in AP is obtained by the proposed SLEEG. The detailed experimental results can be found in the supplementary materials.

4.1.2 Experimental Setup

Implementation Details. For fair comparisons, we follow the similar settings of [14, 25] to utilize the segmentation model of DeepLab series [9] with ResNet101 [19] backbone, which is pre-trained on Cityscapes as in-distribution training and keep fixed without further re-training. The lightweight OoD head consists of three stacked Conv-BN-ReLU blocks and is trained for 40,000 iterations with batchsize of 8, the balance factor is set as $\lambda = 0.5$ for test.

Since the estimated anomalies score is not stable in the beginning and may affect the mask refinement, we apply a warmup strategy for mask refinement. First we take JEM as anomaly score for 6,000 iterations and then replace it with estimated anomaly likelihood. Following common setting [5, 25, 43], the average precision (AP), area under receiver operating characteristics curve (AUROC) and false positive rate (FPR₉₅) at true positive rate of 95% are adopted as metrics to perform comprehensive evaluation. Among these metrics, FPR₉₅ and AP are more crucial since there exists severe imbalance between OoD and ID pixels.

4.2. Experiments Results

4.2.1 Comparison with State-of-the-art Methods

FS Leaderboard. Tab. 1 provides results on test sets of FS benchmark. Following [4], previous methods are categorized based on whether they require re-training the segmentation network or extra OoD data. Compared with previous competitive methods without re-training or OoD data, SLEEG works effectively to outperform most competitors by large margins. Additionally, SLEEG can even surpass some methods with re-training and OoD data by large margins and achieve a new SOTA performance of AP on Lost & Found track, which includes anomalies in more realistic scenes. On the artificially-generated FS Static, SLEEG is on par with the SOTA methods DenseHybrid as well, which requires OoD data and adopts stronger Wide-ResNet38. Although SLEEG is interiors to some methods relying on OoD data in FS Static, this is due to the external data [31] used falls into similar distribution of those utilized for FS static construction [15], thus these methods suffer a large performance gap between artificial Static track and realistic LAF, while SLEEG keeps consistent superiority on both tracks.

FS Validation Sets. Tab. 2 shows comparisons on the validation sets of FS Lost & Found and Static. In terms of AP, our anomaly detector achieves the best results for all metrics on FS Lost & Found and competitive performance on FS Static. Specifically, when compared with GMMSeg [30], SLEEG yields significant improvements of 26.4% on AP and reduce FPR₉₅ to 10.9%. The results demonstrate the effectiveness and robustness of our SLEEG on detecting real-world anomaly instances. Similar to results in Tab. 1, methods with OoD data (*e.g.* PEBAL) or synthetic model (*e.g.* SynthCP) usually suffer from significant performance gap between artificial anomaly in FS Static and anomalies in realistic scenes from LAF, since they tend to overfit abrupt OoD data. In contrast, SLEEG can yield relative consistent performance gain.

Road Anomaly. We further compare our SLEEG with previous SOTA methods on Road Anomaly benchmark in Tab. 2, our approach outperforms most methods by a large margin. Since there exists larger inherent domain shift between Road anomaly and Cityscapes than Fishyscapes, previous methods (*e.g.* GMMSeg [30]) that perform well on Fishyscapes are prone to suffer from poor accuracy on Road anomaly. However, our SLEEG yields significant improvements on both two datasets, demonstrating the robustness of SLEEG in tackling open-world scenes with diverse styles.

4.2.2 Qualitative Results

Figure 4 presents the comparison of the visualization results between pure JEM [16] and our SLEEG, where pixels with yellow and red color are marked as unexpected re-

Estimator		FS LAF Validation			Road Anomaly Validation		
TAE	TORE	FPR ₉₅ ↓	AUROC ↑	AP ↑	FPR ₉₅ ↓	AUROC ↑	AP ↑
✗	✗	27.0	95.5	31.0	76.7	73.1	32.8
✓	✗	25.7	96.2	57.5	32.7	90.0	58.6
✗	✓	18.4	96.9	47.9	35.9	90.0	59.1
✓	✓	10.9	98.3	70.9	28.7	91.1	62.4

Table 3. Ablation results for different likelihood estimators on FS validation set and Road Anomaly validation set.

Margin Type	FS LAF Validation			Road Anomaly Validation		
	FPR ₉₅ ↓	AUROC ↑	AP ↑	FPR ₉₅ ↓	AUROC ↑	AP ↑
Static γ	12.3	97.1	65.2	31.5	89.8	56.0
Dynamic $\hat{\gamma}$	10.9	98.3	70.9	28.7	91.1	62.4

Table 4. Ablation results of comparison between static margin and dynamic margin (Eq. (8)) on FS and Road Anomaly validation set.

Patch Policy	Refinement	FS LAF Validation			Road Anomaly Validation		
		FPR ₉₅ ↓	AUROC ↑	AP ↑	FPR ₉₅ ↓	AUROC ↑	AP ↑
Void as OoD	-	19.3	96.8	47.3	61.2	81.7	46.8
Square Patch	✗	25.4	95.1	45.7	50.6	83.6	40.9
	✓	13.8	97.5	62.5	34.7	90.1	57.4
Convex Patch	✗	13.3	97.9	61.9	37.8	89.4	52.7
	✓	10.9	98.3	70.9	28.7	91.1	62.4

Table 5. Investigation of patch policies on FS and Road Anomaly validation set. “Void as OoD” denotes training models with pixels belonging to void class in Cityscapes as anomaly samples.

gions. Compared with JEM, anomaly scores with greater confidence are generated for OoD samples by SLEEG. The results demonstrates that SLEEG is more capable of tackling the distribution differentiation of inliers and outliers by seamlessly integrating two estimators. Moreover, it can be observed that fewer in-distribution pixels are detected as anomalous ones, resulting in significant reduction in false positive samples. More qualitative results compared with previous methods can be found in supplementary materials.

5. Discussion

5.1. Ablation Study

Effectiveness of Different Estimators. We explore the contribution of TAE and TORE on the anomaly performance of FS Lost & Found and Road Anomaly validation sets. To make comparison, we take the pure JEM [16] as baseline method. It can be observed from Tab. 3 that TAE brings significant improvements to the baseline on the AP by training with self-generated OoD samples. Further, by dynamically adjusting the margin of anomaly scores, TORE brings a large performance boost of around 17% in AP and significant reduction in FPR₉₅ as well. Finally, SLEEG is capable of achieving the best performance by seamlessly integrating two estimators for the prediction of outliers.

Specifically, as indicated by Eq. (8), we also compare the automatic energy-guided margin $\hat{\gamma}$ with a manually tuned

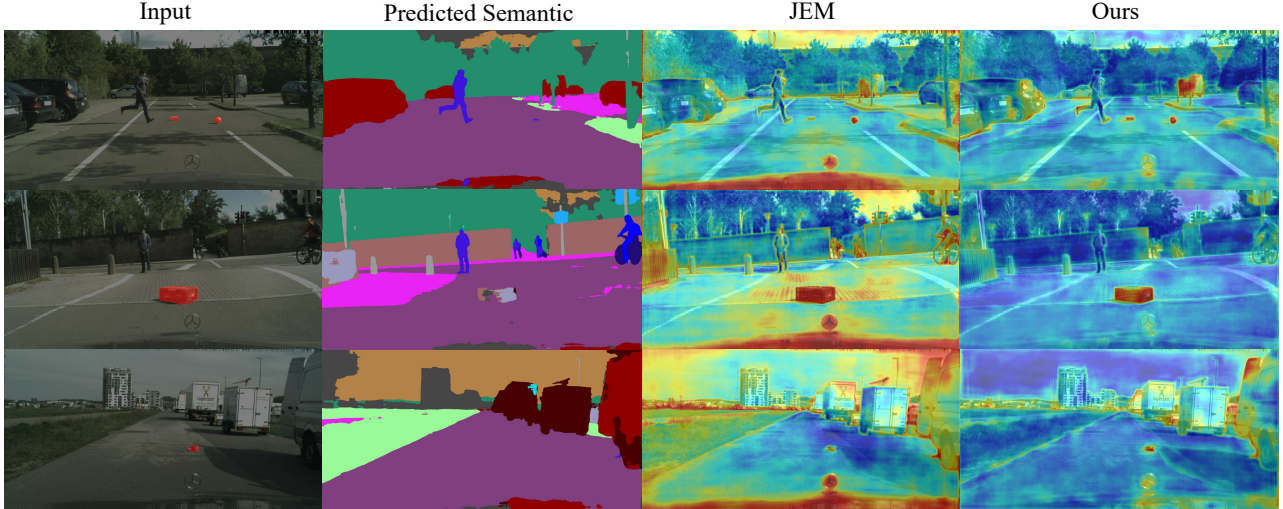


Figure 4. Visualization of on FS Lost & Found validation set. Compared with JEM, predictions from our SLEEG show anomaly maps with higher responses for anomalous instances and lower values for normal pixels.

static value γ for the training of TORE, which is equivalent to eliminating the JEM terms in Eq. (8). For both setting, we set $\gamma = 15$, the results can be illustrated in Tab. 4. It is clear that the margin with a dynamically controlled component as Eq. (8) can consistently outperforms static margin, indicating the residual form of anomaly likelihood can adaptively capture effective training samples.

Investigation on Patch Policy. Tab. 5 shows the comparison results for different patch policies of self-supervised learning on FS Lost & Found validation set and road anomaly validation set. Especially, we design a baseline which regards pixels labeled with “void” from Cityscapes as OoD data (denoted as “Void as OoD”). From Tab. 5, training with simple square patches performs slightly inferior to baseline, since this is prone to implicitly learn useless shape-related prior. With more various shapes, convex patches brings significant improvements. Besides, by performing our refinement strategy, SLEEG can also achieve significant improvement even with simple square patch. Finally, imposing further refinement on the convex patch achieves the best performance.

Parameter Sensitivity. We further investigate the influence of patch number and margin value on the FS Lost & Found validation set. As shown in Fig. 5, SLEEG performs best when margin $\gamma = 15$ and patch number $N = 10$. The results demonstrate that SLEEG achieves similar performance across all settings, implying SLEEG is not very sensitive to both patch number and margin value. Finally, we set patch number and margin to 10 and 15 respectively.

5.2. Extension to More Segmentation Models

Next we also validation the generalization ability of SLEEG by training with different advanced segmentation networks, including OCRNet, ISANet and FCN. As described in Tab. 6, our SLEEG consistently surpasses SML

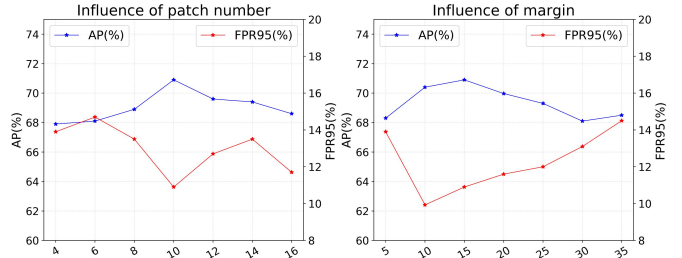


Figure 5. Investigation on the influence on AP and false positive rate with varied patch number N (left) and margin value γ (right) on FS Lost & Found validation set.

Architecture	Method	FS LAF Val		FS Static Val		mIoU
		FPR ₉₅ ↓	AP ↑	FPR ₉₅ ↓	AP ↑	
OCRNet [45]	SML	18.28	39.96	15.07	47.90	80.66
	JEM	22.90	23.27	16.80	34.03	
	Void Class	16.65	46.62	17.74	29.30	
	SLEEG	8.89	72.51	7.6	73.01	
ISANet [24]	SML	18.67	28.76	14.86	32.15	80.51
	JEM	35.57	22.65	16.22	45.22	
	Void Class	29.17	43.53	17.18	24.61	
	SLEEG	12.28	65.79	3.33	80.03	
FCN [39]	SML	39.80	17.59	14.53	28.92	77.72
	JEM	39.36	21.83	13.47	30.51	
	Void Class	24.29	43.44	14.79	22.72	
	SLEEG	21.01	63.11	5.31	61.29	

Table 6. Comparison between SLEEG and other baseline anomaly detection methods on FS validation sets with different segmentation models. “Void Class” denotes training models with pixels that fall into void class as anomaly samples.

and JEM by large margins across all the framework. Additionally, it can be observed that our SLEEG performs better for both AP and FPR₉₅ on FS Lost & Found validation set when adopting networks with higher mIoU scores, implying that SLEEG can work effectively with various segmentation frameworks and bring consistent performance gain.

6. Conclusion

In this paper, we propose SLEEG, a simple and flexible anomaly segmentation framework without requiring re-training or auxiliary OoD data, which exploits a task-agnostic binary estimator and a task-oriented energy residual estimator for anomaly likelihood estimation, and seamlessly incorporate them with an adaptive copy-and-paste mask policy for self-supervised learning. Extensive quantitative and qualitative results on various datasets verify the effectiveness of our approach and a new SOTA performance is achieved on both FS Lost & Found validation and test sets by SLEEG. Finally, SLEEG is also verified effective across various segmentation architectures, demonstrating its great potential in real-world application.

References

- [1] Petra Bevandić, Ivan Krešo, Marin Oršić, and Siniša Šegvić. Discriminative out-of-distribution detection for semantic segmentation. *arXiv preprint arXiv:1808.07703*, 2018. [3](#)
- [2] Petra Bevandić, Ivan Krešo, Marin Oršić, and Siniša Šegvić. Simultaneous semantic segmentation and outlier detection in presence of domain shift. In *German conference on pattern recognition*, pages 33–47. Springer, 2019. [2](#), [3](#)
- [3] Petra Bevandić, Ivan Krešo, Marin Oršić, and Siniša Šegvić. Dense outlier detection and open-set recognition based on training with noisy negative images. *arXiv preprint arXiv:2101.09193*, 2021. [4](#), [6](#)
- [4] Hermann Blum, Paul-Edouard Sarlin, Juan Nieto, Roland Siegwart, and Cesar Cadena. Fishyscapes: A benchmark for safe semantic segmentation in autonomous driving. In *Proc. of the IEEE/CVF International Conference on Computer Vision Workshops*, pages 0–0, 2019. [2](#), [7](#)
- [5] Hermann Blum, Paul-Edouard Sarlin, Juan Nieto, Roland Siegwart, and Cesar Cadena. The fishyscapes benchmark: Measuring blind spots in semantic segmentation. *International Journal of Computer Vision*, 129(11):3119–3135, 2021. [5](#), [6](#)
- [6] Daniel Bogdoll, Maximilian Nitsche, and J Marius Zöllner. Anomaly detection in autonomous driving: A survey. In *Proc. IEEE Conference on Computer Vision and Pattern Recognition (CVPR)*, pages 4488–4499, 2022. [2](#), [3](#)
- [7] Robin Chan, Krzysztof Lis, Svenja Uhlemeyer, Hermann Blum, Sina Honari, Roland Siegwart, Mathieu Salzmann, Pascal Fua, and Matthias Rottmann. Segmentmeifyoucan: A benchmark for anomaly segmentation. *NeurIPS 2021-Dataset Track*, 2021. [2](#), [5](#)
- [8] Robin Chan, Matthias Rottmann, and Hanno Gottschalk. Entropy maximization and meta classification for out-of-distribution detection in semantic segmentation. In *Proc. IEEE International Conference on Computer Vision (ICCV)*, pages 5128–5137, 2021. [2](#), [3](#)
- [9] Liang-Chieh Chen, Yukun Zhu, George Papandreou, Florian Schroff, and Hartwig Adam. Encoder-decoder with atrous separable convolution for semantic image segmentation. In *Proc. European Conference on Computer Vision (ECCV)*, pages 801–818, 2018. [1](#), [2](#), [6](#)
- [10] Marius Cordts, Mohamed Omran, Sebastian Ramos, Timo Rehfeld, Markus Enzweiler, Rodrigo Benenson, Uwe Franke, Stefan Roth, and Bernt Schiele. The cityscapes dataset for semantic urban scene understanding. In *Proc. IEEE Conference on Computer Vision and Pattern Recognition (CVPR)*, pages 3213–3223, 2016. [1](#), [2](#), [3](#), [5](#)
- [11] Antonia Creswell, Tom White, Vincent Dumoulin, Kai Arulkumaran, Biswa Sengupta, and Anil A Bharath. Generative adversarial networks: An overview. *IEEE signal processing magazine*, 35(1):53–65, 2018. [3](#)
- [12] Akshay Raj Dhamija, Manuel Günther, and Terrance Boulton. Reducing network agnostophobia. *Proc. Advances in Neural Information Processing Systems (NeurIPS)*, 31, 2018. [2](#)
- [13] Giancarlo Di Biase, Hermann Blum, Roland Siegwart, and Cesar Cadena. Pixel-wise anomaly detection in complex driving scenes. In *Proc. IEEE Conference on Computer Vision and Pattern Recognition (CVPR)*, pages 16918–16927, 2021. [2](#), [4](#), [6](#)
- [14] Giancarlo Di Biase, Hermann Blum, Roland Siegwart, and Cesar Cadena. Pixel-wise anomaly detection in complex driving scenes. In *Proc. IEEE Conference on Computer Vision and Pattern Recognition (CVPR)*, pages 16918–16927, 2021. [3](#), [6](#)
- [15] Mark Everingham, Luc Van Gool, Christopher KI Williams, John Winn, and Andrew Zisserman. The pascal visual object classes (voc) challenge. *International journal of computer vision*, 88(2):303–338, 2010. [5](#), [7](#)
- [16] Will Grathwohl, Kuan-Chieh Wang, Joern-Henrik Jacobsen, David Duvenaud, Mohammad Norouzi, and Kevin Swersky. Your classifier is secretly an energy based model and you should treat it like one. In *Proc. International Conference on Learning Representations (ICLR)*, 2020. [2](#), [3](#), [4](#), [7](#)
- [17] Matej Grcić, Petra Bevandić, and Siniša Šegvić. Densehybrid: Hybrid anomaly detection for dense open-set recognition. *arXiv preprint arXiv:2207.02606*, 2022. [1](#), [2](#), [4](#), [6](#)
- [18] Chris Harris, Mike Stephens, et al. A combined corner and edge detector. In *Alvey vision conference*, volume 15, pages 10–5244. Manchester, UK, 1988. [5](#)
- [19] Kaiming He, Xiangyu Zhang, Shaoqing Ren, and Jian Sun. Deep residual learning for image recognition. In *Proc. IEEE Conference on Computer Vision and Pattern Recognition (CVPR)*, pages 770–778, 2016. [6](#)
- [20] Dan Hendrycks, Steven Basart, Mantas Mazeika, Mohammadreza Mostajabi, Jacob Steinhardt, and Dawn Song. Scaling out-of-distribution detection for real-world settings. *arXiv preprint arXiv:1911.11132*, 2019. [6](#)
- [21] Dan Hendrycks and Kevin Gimpel. A baseline for detecting misclassified and out-of-distribution examples in neural networks. *arXiv preprint arXiv:1610.02136*, 2016. [2](#)
- [22] Dan Hendrycks and Kevin Gimpel. A baseline for detecting misclassified and out-of-distribution examples in neural networks. *Proc. International Conference on Learning Representations (ICLR)*, 2017. [1](#), [6](#)
- [23] Dan Hendrycks, Mantas Mazeika, and Thomas Dietterich. Deep anomaly detection with outlier exposure. *arXiv preprint arXiv:1812.04606*, 2018. [2](#), [3](#)

- [24] Lang Huang, Yuhui Yuan, Jianyuan Guo, Chao Zhang, Xilin Chen, and Jingdong Wang. Interlaced sparse self-attention for semantic segmentation. *arXiv preprint arXiv:1907.12273*, 2019. 8
- [25] Sanghun Jung, Jungsoo Lee, Daehoon Gwak, Sungha Choi, and Jaegul Choo. Standardized max logits: A simple yet effective approach for identifying unexpected road obstacles in urban-scene segmentation. In *Proc. IEEE International Conference on Computer Vision (ICCV)*, pages 15425–15434, 2021. 2, 6
- [26] Balaji Lakshminarayanan, Alexander Pritzel, and Charles Blundell. Simple and scalable predictive uncertainty estimation using deep ensembles. *Proc. Advances in Neural Information Processing Systems (NeurIPS)*, 30, 2017. 2
- [27] Yann LeCun, Sumit Chopra, Raia Hadsell, M Ranzato, and F Huang. A tutorial on energy-based learning. *Predicting structured data*, 1(0), 2006. 2, 3
- [28] Kimin Lee, Honglak Lee, Kibok Lee, and Jinwoo Shin. Training confidence-calibrated classifiers for detecting out-of-distribution samples. *arXiv preprint arXiv:1711.09325*, 2017. 2
- [29] Kimin Lee, Kibok Lee, Honglak Lee, and Jinwoo Shin. A simple unified framework for detecting out-of-distribution samples and adversarial attacks. *Proc. Advances in Neural Information Processing Systems (NeurIPS)*, 31, 2018. 2
- [30] Chen Liang, Wenguan Wang, Jiaxu Miao, and Yi Yang. Gmmseg: Gaussian mixture based generative semantic segmentation models. *arXiv preprint arXiv:2210.02025*, 2022. 6, 7
- [31] Tsung-Yi Lin, Michael Maire, Serge Belongie, James Hays, Pietro Perona, Deva Ramanan, Piotr Dollár, and C Lawrence Zitnick. Microsoft coco: Common objects in context. In *Proc. European Conference on Computer Vision (ECCV)*, pages 740–755. Springer, 2014. 2, 3, 7
- [32] Krzysztof Lis, Krishna Nakka, Pascal Fua, and Mathieu Salzmann. Detecting the unexpected via image resynthesis. In *Proc. IEEE International Conference on Computer Vision (ICCV)*, pages 2152–2161, 2019. 3
- [33] Krzysztof Lis, Krishna Nakka, Pascal Fua, and Mathieu Salzmann. Detecting the unexpected via image resynthesis. In *Proc. IEEE International Conference on Computer Vision (ICCV)*, 2019. 6
- [34] Andrey Malinin and Mark JF Gales. Predictive uncertainty estimation via prior networks. In *Proc. Advances in Neural Information Processing Systems (NeurIPS)*, 2018. 1, 6
- [35] Jishnu Mukhoti and Yarin Gal. Evaluating bayesian deep learning methods for semantic segmentation. *arXiv preprint arXiv:1811.12709*, 2018. 1, 6
- [36] Nobuyuki Otsu. A threshold selection method from gray-level histograms. *IEEE transactions on systems, man, and cybernetics*, 9(1):62–66, 1979. 5
- [37] Peter Pinggera, Sebastian Ramos, Stefan Gehrig, Uwe Franke, Carsten Rother, and Rudolf Mester. Lost and found: detecting small road hazards for self-driving vehicles. In *2016 IEEE/RSJ International Conference on Intelligent Robots and Systems (IROS)*, pages 1099–1106. IEEE, 2016. 5, 6
- [38] Olga Russakovsky, Jia Deng, Hao Su, Jonathan Krause, Sanjeev Satheesh, Sean Ma, Zhiheng Huang, Andrej Karpathy, Aditya Khosla, Michael Bernstein, et al. Imagenet large scale visual recognition challenge. *International journal of computer vision*, 115(3):211–252, 2015. 3
- [39] Evan Shelhamer, Jonathan Long, and Trevor Darrell. Fully convolutional networks for semantic segmentation. *IEEE Transactions on Pattern Analysis and Machine Intelligence (TPAMI)*, 39(4):640–651, 2017. 8
- [40] Yiyao Sun, Yifei Ming, Xiaojin Zhu, and Yixuan Li. Out-of-distribution detection with deep nearest neighbors. *arXiv preprint arXiv:2204.06507*, 2022. 2
- [41] Yu Tian, Yuyuan Liu, Guansong Pang, Fengbei Liu, Yuanhong Chen, and Gustavo Carneiro. Pixel-wise energy-biased abstention learning for anomaly segmentation on complex urban driving scenes. *arXiv preprint arXiv:2111.12264*, 2021. 1, 3, 4, 6
- [42] Tomas Vojir, Tomáš Šipka, Rahaf Aljundi, Nikolay Chumerin, Daniel Olmeda Reino, and Jiri Matas. Road anomaly detection by partial image reconstruction with segmentation coupling. In *Proc. IEEE International Conference on Computer Vision (ICCV)*, pages 15651–15660, 2021. 2
- [43] Yingda Xia, Yi Zhang, Fengze Liu, Wei Shen, and Alan L Yuille. Synthesize then compare: Detecting failures and anomalies for semantic segmentation. In *Proc. European Conference on Computer Vision (ECCV)*, pages 145–161. Springer, 2020. 2, 3, 6
- [44] Yijun Yang, Ruiyuan Gao, and Qiang Xu. Out-of-distribution detection with semantic mismatch under masking. *arXiv preprint arXiv:2208.00446*, 2022. 2
- [45] Yuhui Yuan, Xilin Chen, and Jingdong Wang. Object-contextual representations for semantic segmentation. 2020. 8
- [46] Yibo Zhou. Rethinking reconstruction autoencoder-based out-of-distribution detection. In *Proc. IEEE Conference on Computer Vision and Pattern Recognition (CVPR)*, pages 7379–7387, 2022. 2
- [47] Bo Zong, Qi Song, Martin Renqiang Min, Wei Cheng, Cristian Lumezanu, Daeki Cho, and Haifeng Chen. Deep autoencoding gaussian mixture model for unsupervised anomaly detection. In *Proc. International Conference on Learning Representations (ICLR)*, 2018. 2